SUPPLEMENTARY INFORMATION

SUPPLEMENTARY EXPERIMENTAL PROCEDURES

RNA extraction and quantitative PCR

Nuclear/cytoplasmic fractionation was performed as described (Harrow et al., 2012). RNA from nuclear and cytoplasmic fractions or total RNA form GSCs and patients' tissues was extracted using TRIzol (Ambion). RNA from formalin fixed sections of mouse xenograft tumors was extracted with PureLink FFPE (Invitrogen) following the manufactures' instructions. RNA was reverse-transcribed using iScript cDNA Synthesis Kit (BioRad) and gene expression analyzed by qPCR using Power SYBR Green PCR Master Mix (Applied Biosystems). List of primers used throughout the study:

Primer name	Primer sequence	Primer name	Primer sequence
18S For	AACTTTCGATGGTAGTCGCCG	LYN For	TTCCCTACCCAGGGAGAACT
18S Rev	CCTTGGATGTGGTAGCCGTTT	LYN Rev	CTGCCTTTTCTTTCCAGCAC
ADM For	GGTCGGACTCTGGTGTCTTC	MALAT1 For	AGCAGACACACGTATGCGAA
ADM Rev	GCTTGCGCGACTATTCCTTG	MALAT1 Rev	GTGGTTCCCAATCCCCACAT
BCL2A1 For	AAATTGCCCCGGATGTGGAT	MEG3 For	GCAGGATCTGGCATAGAGGA
BCL2A1 Rev	ACAAAGCCATTTTCCCAGCC	MEG3 Rev	TTGGCTGATGCAAGGAGAG
CAV2 For	CCTGCCTAATGGTTCTGCCT	MET For	TAGCCAACCGAGAGACAAGC
CAV2 Rev	CTCAGTTGCAGGCTGACAGA	MET Rev	TGTGCTCCCACCACTAATAAAAG
CD133 For	GCAATCTCCCTGTTGGTGAT	NDRG1 For	GGCACCGTCCTTTCCTTTCT
CD133 Rev	CCAGTTTCCGACTCCTTTTG	NDRG1 Rev	GAGTACGCGGGGCTACAAA
CD44 For	AAGGTGGAGCAAACACAACC	NDUFAF4 For	GACACCCCTCTACCAACAGC
CD44 Rev	CTTCTGCCCACACCTTCTTC	NDUFAF4 Rev	ACCTGCAAGGAAGACACAGG
DHX9 For	GCCAATTTCTGGCCAAAGCA	NEAT1 For	GCTTTGCTACAAGGTGGGGA
DHX9 Rev	CGAGGCTCAATGGGGAGTTT	NEAT1 Rev	CACCCCTCCCTTTGGTTCTC
DLEU2 For	CGGGTACTTATCTCCGACCTC	Nestin For	CCCCGTCGGTCTCTTTTCTC
DLEU2 Rev	TCCAGGGAAGGATGTAGCTG	Nestin Rev	TCGTCTGACCCACTGAGGAT
EPAS1 For	GTCCCACCAGCTTCACTCTC	NOTCH1 For	TCACGCTGACGGAGTACAAG
EPAS1 Rev	GGCAAGTCTGCCAGGTAAGT	NOTCH1 Rev	GGCAGTGGCAGATGTAGGAG
ERO1A For	GGCTTCTGGTCAAGGGACAA	OLIG2 For	GTTCTCCCCTGAGGCTTTTC
ERO1A Rev	TGCTTGCATGTAGGCCAGATA	OLIG2 Rev	GGAAGATAGTCGTCGCAGCTT
FOSL1 For	GTCTTCACCTACCCCAGCAC	PFKP For	AAGTTCCTGGAGCACCTCTC
FOSL1 Rev	CTCACAAAGCGAGGAGGGTT	PFKP Rev	GTAGATACCCATGCGCACCA
GAS5 For	GGTATGGAGAGTCGGCTTGA	POPDC3 For	TGCACAACCTGGAAGCAAGA
GAS5 Rev	TGCATGCTTGCTTGTTGTGG	POPDC3 Rev	AGAAAACCCAACCCCAGCAA
GPR160 For	ACTTGCGCAAATGTCTCCGA	PRNCR1 For	TGCCCATCTCCTGATCAACC
GPR160 Rev	TGTCCTCTCCAGTGGGTCTT	PRNCR1 Rev	TCTGAAGTTGTTGCGGTCAGT
HIF1A For	TTCCTTCTCTTCTCCGCGTG	RMRP For	CACGTAGACATTCCCCGCTT
HIF1A Rev	TTTTCTTGTCGTTCGCGCC	RMRP Rev	CTGCCTGCGTAACTAGAGGG
HIF1AAS2 For	AAAGCTTGGGCAAATTATTCA	SDC4 For	TACTTCTCCGGAGCCCTACC
HIF1AAS2 Rev	TGAATGGGATGAGTGAAGCA	SDC4 Rev	AACTTCAGGGCCGATCATGG
HMGA1 For	CAGCTTCCTTCTGGGACTGG	SLC2A1 For	TGTGTATGCCACCATTGGCT
HMGA1 Rev	GTGTAGTGTGGTGGTGAGGG	SLC2A1 Rev	CTAGCGCGATGGTCATGAGT
HMGA2 For	GCCCTCTCCTAAGAGACCCA	SOX2 For	CCTGATTCCAGTTTGCCTCT
HMGA2 Rev	CTGCCTCTTGGCCGTTTTTC	SOX2 Rev	CAGCTCCGTCTCCATCATGT
IGF2 For	CGTCCCCTGATTGCTCTACC	TAF9B For	ATAGCAACCCCACAAACGGT
IGF2 Rev	CGGCAGTTTTGCTCACTTCC	TAF9B Rev	GGTGTGGACTGAGAAGGTGG
IGF2BP2 For	ACACAGACACAGAAACCGCC	WT1 For	ACTCTTGTACGGTCGGCATC
IGF2BP2 Rev	AACTGATGCCCGCTTAGCTT	WT1 Rev	TCTCACCAGTGTGCTTCCTG
IGFBP3 For	CGCCAGGAAATGCTAGTGAG	WT1-AS For	CCACCACCCCTCTACCTCTT
IGFBP3 Rev	AACTTGGGATCAGACACCCG	WT1-AS Rev	CCTACCCAGCCTCGATTTTT

In vivo Magnetic Resonance Imaging

Studies were performed using a 7.0T Bruker BioSpec USR (Bruker BioSpin Corp.) in the Small Animal Imaging Laboratory (SAIL) at the Brigham and Women's Hospital. Isoflurane was used as anesthetic at a

level of 1.5%, and heart and respiratory rates were monitored. Rapid acquisition with relaxation enhancement T2-weighted imaging was performed with the following parameters: echo time=8.8 ms, repetition time=6466 ms, field of view=2.5 cm x 2.5 cm, matrix size of 250 x 250, and a spatial resolution of 100 μm x 100 μm isotropic. The total scan time was 26 minutes and 43 seconds per animal. 3D reconstruction of animal brains was performed using Osirix Lite Version 7.0.

Cell assays

GSCs were plated in supplemented Neurobasal medium at the concentration of 40,000 cells/mL and incubated for 96 h. After incubation, cells were counted and analyzed for viability using the Muse Count & Viability Reagent on the Muse Cell Analyzer (Millipore) following the manufactures' instructions.

For spheroid formation GSCs were dissociated to single cells and plated at 500 cells/well in 96-well plate in 100 µl supplemented Neurobasal. Size of spheroids was quantified after 96 h using ImageJ. For limited dilution spheroid assay single cell suspension were plated in ultra-low attachment 96-well plates at different concentrations (from 1 to 500 cells per well) in 0.1ml of supplemented Neurobasal medium. Cultures were left undisturbed for 7 days. After incubation, spheres were imaged using a microscope Nikon eclipse Ti, percentage of wells not containing spheres for each cell concentration was calculated and plotted against the number of cells per well.

SUPPLEMENTARY FIGURE LEGEND

Figure S1. Supplementary to Figure 1.
A. Gene signature distinguishes proneural (blue) from mesenchymal (red) GSCs. Gene sets that vary coherently between GSCs were validated by qPCR data and used for subtype classification by clustering. Non classified GSCs and normal human astrocytes (AST) (black) are also shown.
B. GBM and GSC lncRNA profile distinguishes tumor (Tumor Tissue - TT) from normal tissue (matched Tissue Adjacent to brain Tumor - TAT) and proneural (blue) from mesenchymal (red) GSC subtypes. LncRNA sets that vary coherently between tissues (left) and GSCs (right) were identified by unsupervised clustering. Normal human astrocytes (AST) (black) are also shown.
C. Expression of selected lncRNAs in GSC validates the global profiling. Relative expression based on qPCR in proneural (blue) and mesenchymal (red) GSC is shown. Data shown as mean ±SD, * P value < 0.05, ns – non-significant P value.

Figure S2. Supplementary to Figure 2.
A. Knockdown of HIF1A-AS2 reduces viability of mesenchymal GSCs. Representative cell viability profiles are shown.
B. Knockdown of HIF1A-AS2 reduces GSC proliferation and viability. qPCR analysis (left) and cell number and percentage of dead cells (right) in mesenchymal (M) and proneural (P) GSC are shown. Data shown as mean ±SD, * P value < 0.05, * P value < 0.01
C. Knockdown of HIF1A-AS2 results in gene expression rearrangement. Expression of 730 cancer-related genes in control and HIF1A-AS2 knockdown mesenchymal GSC (two single cell clones #1 and #2 were analyzed) were analyzed by unsupervised clustering (top panel). The mesenchymal (M) and proneural (P) GSC-specific genes were analyzed with HIF1A-AS2 knockdown signature by supervised clustering (bottom panel).
D. The gene expression analysis indicates diverse molecular modules deregulated in mesenchymal GSC upon HIF1A-AS2 knockdown and predict patient outcome. Genes significantly deregulated by HIF1A-AS2 knockdown in M GSCs were analyzed by Gene Ontology enrichment in indicated subcategories
E. Genes deregulated upon HIF1A-AS2 knockdown predict patient outcome. Survival analysis based on the impact of the prognostic index of multiple genes (See Supplementary Table 2) down-regulated by HIF1A-AS2 knockdown in mesenchymal (M) GSC is shown in full cohort and in classical (C), mesenchymal (M) and neural (N) subclasses.
F. Mesenchymal and proneural GSC responds to hypoxia *via* up-regulation of HIF1α and EPAS1 proteins. QPCR (left) and Western blot (right) analysis is shown. Data shown as mean ±SD.
G. Effect of hypoxia on proliferation (left) and viability (right) of GSCs. Cell number and percentage of dead cells are shown. Proneural (P) GSC n=3, mesenchymal (M) GSC n=3. Data shown as mean ±SD, * P value < 0.05.
H. HIF1A-AS2 is upregulated upon exposure to hypoxia in differentiated GBM cells. QPCR of GFAP (left) and HIF1A-AS2 (right) is shown. Data shown as mean ±SD.
I. Knockdown of HIF1A-AS2 reduces proliferation (left) and viability (right) of differentiated GBM cells. Cell number and percentage of dead cells are shown. Data shown as mean ±SD, * P value < 0.05".**J.** Hypoxia-dependent induction of endogenous HIF1A-AS2 overcomes the shRNA effect. QPCR analysis is shown. Data shown as mean ±SD.
K. HIF1A-AS2 is localized predominantly in the nucleus. QPCR analysis of HIF1A-AS2, MALAT1 and GAPDH is shown. Data shown as mean ±SD.

Figure S3. Supplementary to Figure 3.
A. HIF1A-AS2 knockdown reduces tumor volume. Representative photographs of resected brains (left), consecutive MRI sections (middle) and 3D MRI reconstruction of brain tumor (right) 10 days post implantation are shown.

Figure S4. Supplementary to Figure 4.

A. HIF1A-AS2 interactome network regulate posttranscriptional regulation of gene expression and mRNA stabilization. HIF1A-AS2 partners were identified by pulldown/MS strategy. Networking was analyzed with STRING software (left) and Gene Ontology Biological processes (right)

B. DHX9 and IGF2BP2 are specific partners of HIF1A-AS2. Analysis of UV-crosslinked α-DHX9 RIP (left) and α-IGF2BP2 RIP (right). QPCR analysis on selected proneural (blue), mesenchymal (red) or non-subtype specific (black) lncRNAs in mesenchymal GSCs is shown. Data shown as mean ±SD, ** P value < 0.01.

C. Mesenchymal GSC overexpressed IGF2BP2 target genes correlate with mesenchymal subtype. Genes that vary coherently between proneural and mesenchymal GSCs from IGF2BP2 targets signature (n=277) were retrieved from TCGA GBM dataset and identified by class (classical (C), mesenchymal (M) and proneural (P) neural (N) subclasses) (top) and clustering (bottom).

D. HMGA1 and FOSL1 are targets of both HIF1A-AS2 interacting partners. Venn diagram depicting genes identified as IGF2BP targets and its expression in proneural (P) and mesenchymal (M) GSC (left) or its expression in HIF1A-AS2 and DHX9 knockdown (right).

E. Expression of DHX9 and IGF2BP2 downstream genes is up-regulated in mesenchymal GSCs. QPCR analysis of selected genes in proneural (P) and mesenchymal (M) GSCs (left) and in HIF1A-AS2 knockdown M GSCs (right) by qPCR is shown. Data shown as mean ±SD.

F. Knockdown of HIF1A-AS2 in mesenchymal GSCs reduces levels of HMGA1 mRNA. QPCR analysis of selected genes in mesenchymal GSCs upon HIF1A-AS2 knockdown is shown. Expression is relative to control mesenchymal GSCs. Data shown as mean ±SD.

G. HMGA1 is mesenchymal GSC-enriched factor. Western blot analysis of selected proteins in P and M GSCs is shown.

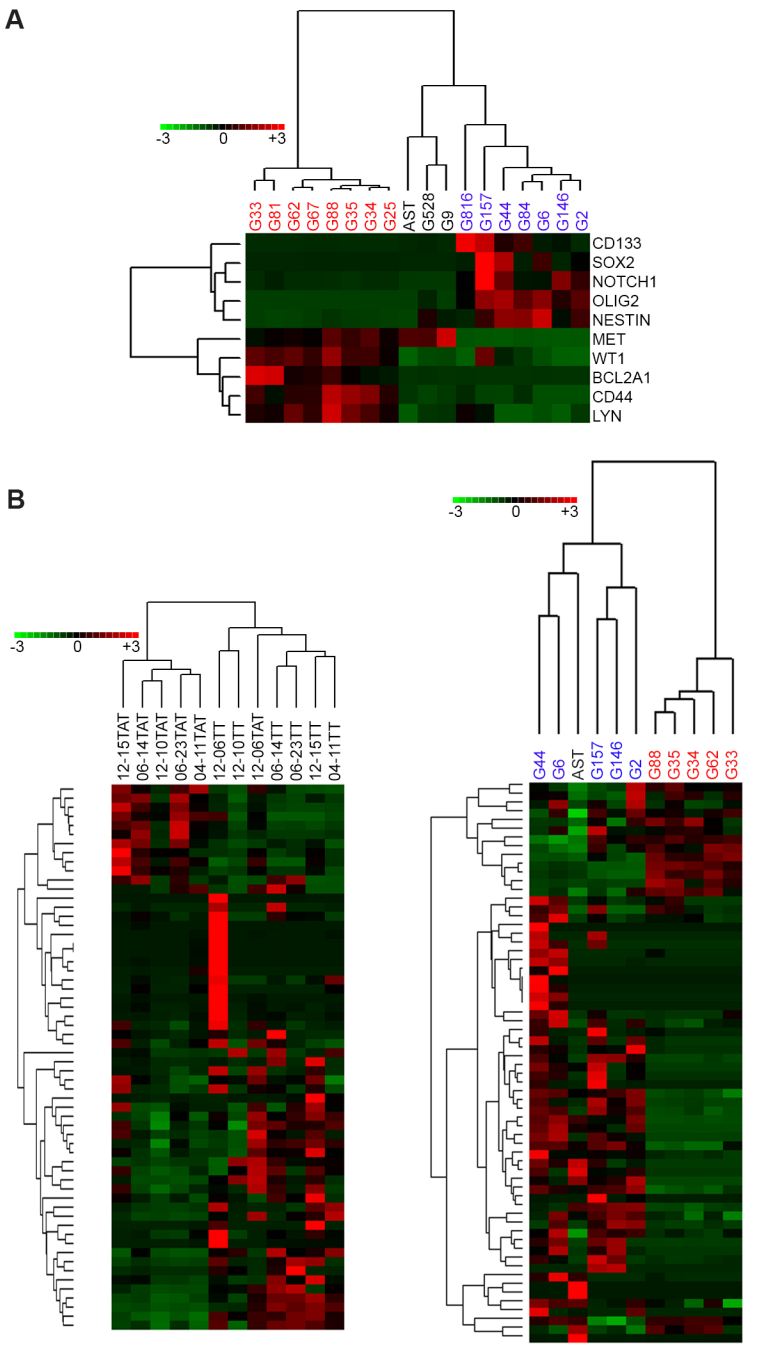
A
-3
0
+3
G33
G81
G62
G67
G88
G35
G34
G25
AST
G528
G9
G816
G157
G44
G84
G6
G146
G2
CD133
SOX2
NOTCH1
OLIG2
NESTIN
MET
WT1
BCL2A1
CD44
LYN
B
-3
0
+3
12-15TAT
06-14TAT
12-10TAT
06-23TAT
04-11TAT
12-06TT
12-10TT
12-06TAT
06-14TT
06-23TT
12-15TT
04-11TT
-3
0
+3
G44
G6
AST
G157
G146
G2
G88
G35
G34
G62
G33
C
Relative MEG3 level
**
G157
G44
G146
G6
G2
G88
G62
G35
G34
G33
Relative WT1-AS level
**
G157
G44
G146
G6
G2
G88
G62
G35
G34
G33
Relative MALAT1 level
ns
G157
G44
G146
G6
G2
G88
G62
G35
G34
G33

Figure S1

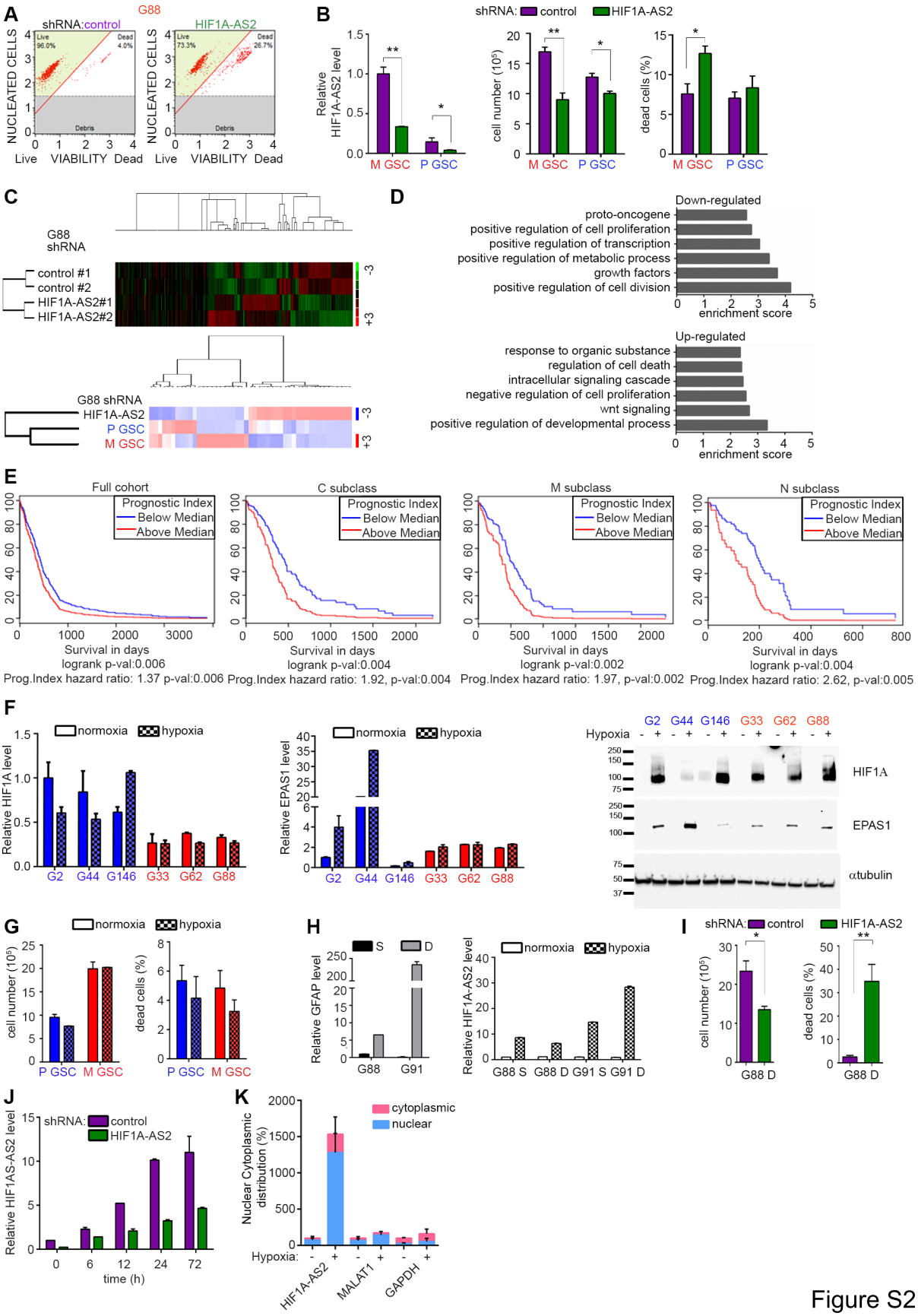
A
G88
shRNA:control
HIF1A-AS2
NUCLEATED CELLS
Live
Dead
Debris
VIABILITY
B
shRNA: control HIF1A-AS2
Relative HIF1A-AS2 level
cell number (10^5)
dead cells (%)
M GSC
P GSC
C
G88 shRNA
control #1
control #2
HIF1A-AS2#1
HIF1A-AS2#2
G88 shRNA
HIF1A-AS2
P GSC
M GSC
D
Down-regulated
proto-oncogene
positive regulation of cell proliferation
positive regulation of transcription
positive regulation of metabolic process
growth factors
positive regulation of cell division
enrichment score
Up-regulated
response to organic substance
regulation of cell death
intracellular signaling cascade
negative regulation of cell proliferation
wnt signaling
positive regulation of developmental process
enrichment score
E
Full cohort
C subclass
M subclass
N subclass
Prognostic Index
Below Median
Above Median
Survival in days
logrank p-val:0.006
Prog.Index hazard ratio: 1.37 p-val:0.006
logrank p-val:0.004
Prog.Index hazard ratio: 1.92, p-val:0.004
logrank p-val:0.002
Prog.Index hazard ratio: 1.97, p-val:0.002
logrank p-val:0.004
Prog.Index hazard ratio: 2.62, p-val:0.005
F
normoxia
hypoxia
Relative HIF1A level
Relative EPAS1 level
G2
G44
G146
G33
G62
G88
Hypoxia
HIF1A
EPAS1
αtubulin
G
normoxia
hypoxia
cell number (10^5)
dead cells (%)
P GSC
M GSC
H
S
D
Relative GFAP level
G88
G91
normoxia
hypoxia
Relative HIF1A-AS2 level
G88 S
G88 D
G91 S
G91 D
I
shRNA: control HIF1A-AS2
cell number (10^5)
dead cells (%)
G88 D
J
shRNA: control HIF1A-AS2
Relative HIF1AS-AS2 level
time (h)
K
cytoplasmic
nuclear
Nuclear Cytoplasmic distribution (%)
Hypoxia:
HIF1A-AS2
MALAT1
GAPDH

Figure S2

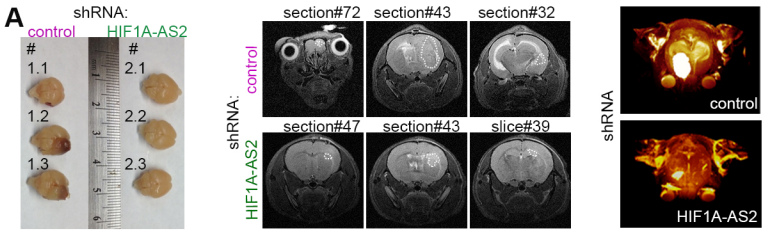
A
shRNA:
control
HIF1A-AS2
#
1.1
1.2
1.3
#
2.1
2.2
2.3
shRNA:
control
HIF1A-AS2
section#72
section#43
section#32
section#47
section#43
slice#39
shRNA
control
HIF1A-AS2

Figure S3

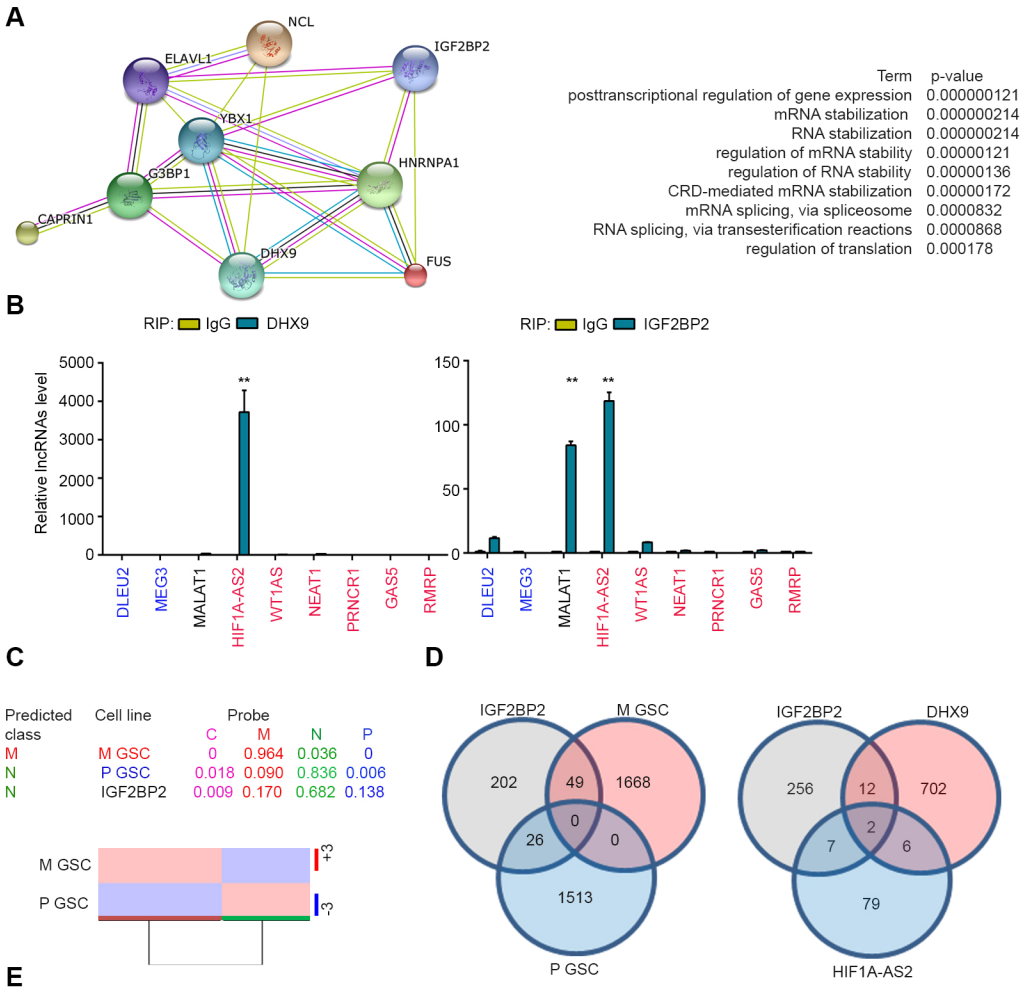
A
NCL
IGF2BP2
ELAVL1
YBX1
HNRNPA1
G3BP1
CAPRIN1
DHX9
FUS
Term p-value
posttranscriptional regulation of gene expression 0.000000121
mRNA stabilization 0.000000214
RNA stabilization 0.000000214
regulation of mRNA stability 0.00000121
regulation of RNA stability 0.00000136
CRD-mediated mRNA stabilization 0.00000172
mRNA splicing, via spliceosome 0.0000832
RNA splicing, via transesterification reactions 0.0000868
regulation of translation 0.000178
B
RIP: IgG DHX9
RIP: IgG IGF2BP2
Relative lncRNAs level
DLEU2
MEG3
MALAT1
HIF1A-AS2
WT1AS
NEAT1
PRNCR1
GAS5
RMRP
C
Predicted class
Cell line
Probe
C M N P
M M GSC 0 0.964 0.036 0
N P GSC 0.018 0.090 0.836 0.006
N IGF2BP2 0.009 0.170 0.682 0.138
M GSC
P GSC
D
IGF2BP2
M GSC
202
49
1668
0
26
0
1513
P GSC
IGF2BP2
DHX9
256
12
702
2
7
6
79
HIF1A-AS2
E
GSC: P M
Relative expression level
DHX9
IGF2BP2
IGF2
HMGA1
FOSL1
CAV2
NDUFAF4
GPR160
TAF9B
POPDC3
HMGA2
shRNA: control HIF1A-AS2
F
G33
Relative expression level
DHX9
IGF2BP2
HMGA1
G
G2
G44
G146
G33
G62
G88
DHX9
IGF2BP2
HMGA1
αtubulin

Figure S4

SUPPLEMENTARY TABLE LEGEND

Table S1. Supplementary to Figure 1B. List of lncRNA transcripts used for Nanostring platform. (See Excel file)
Table S2. Supplementary to Figure 2E. List of genes that vary coherently between control and HIF1A-AS2 knockdown M GSC. (See Excel file)
Table S3. Supplementary to Figure 4A. List of HIF1A-AS2 interacting proteins identified by mass spectrometry. (See Excel file)
Table S4. Supplementary to Figure 4F. List of genes used to query Ivy GAP database

Gene symbol	Gene name	Gene ID	Chromosome
PROM1 (CD133)	prominin 1	8842	4
OLIG2	oligodendrocyte lineage transcription factor 2	10215	21
NOTCH1	notch 1	4851	9
SOX2	SRY (sex determining region Y)-box 2	6657	3
NES	nestin	10763	1
CD44	CD44 molecule (Indian blood group)	960	11
LYN	v-yes-1 Yamaguchi sarcoma viral related oncogene homolog	4067	8
BCL2A1	BCL2-related protein A1	597	15
WT1	Wilms tumor 1	7490	11
MET	met proto-oncogene (hepatocyte growth factor receptor)	4233	7
SDC4	syndecan 4	6385	20
IGFBP3	insulin-like growth factor binding protein 3	3486	7
ERO1L	ERO1-like (S. cerevisiae)	30001	14
PGK1	phosphoglycerate kinase 1	5230	X
ADM	adrenomedullin	133	11
NDRG1	N-myc downstream regulated 1	10397	8
VEGFA	vascular endothelial growth factor A	7422	6
PFKP	phosphofructokinase, platelet	5214	10
SLC2A1	solute carrier family 2 (facilitated glucose transporter), member 1	6513	1
PDK1	pyruvate dehydrogenase kinase, isozyme 1	5163	2
ITGA3	integrin, alpha 3	3675	17
FOSL1	FOS-like antigen 1	8061	11
HMGA1	high mobility group AT-hook 1	3159	6
HMGA2	high mobility group AT-hook 2	8091	12
KLF4	Kruppel-like factor 4 (gut)	9314	9
FGF5	fibroblast growth factor 5	2250	4
GADD45B	growth arrest and DNA-damage-inducible, beta	4616	19
RPS27A	ribosomal protein S27a	6233	2
COL27A1	collagen, type XXVII, alpha 1	85301	9
IL12A	interleukin 12A	3592	3

SUPPLEMENTARY REFERENCES

Ahn, S., Huang, C.L., Ozkumur, E., Zhang, X., Chinnala, J., Yalcin, A., Bandyopadhyay, S., Russek, S., Unlu, M.S., DeLisi, C., *et al.* (2012). TATA binding proteins can recognize nontraditional DNA sequences. Biophysical journal *103*, 1510-1517.

Anney, R.J., Lasky-Su, J., O'Dushlaine, C., Kenny, E., Neale, B.M., Mulligan, A., Franke, B., Zhou, K., Chen, W., Christiansen, H., *et al.* (2008). Conduct disorder and ADHD: evaluation of conduct problems as a categorical and quantitative trait in the international multicentre ADHD genetics study. American journal of medical genetics Part B, Neuropsychiatric genetics : the official publication of the International Society of Psychiatric Genetics *147B*, 1369-1378.

Arora, R., Brun, C.M., and Azzalin, C.M. (2011). TERRA: Long Noncoding RNA at Eukaryotic Telomeres. Progress in molecular and subcellular biology *51*, 65-94.

Beltran, M., Puig, I., Pena, C., Garcia, J.M., Alvarez, A.B., Pena, R., Bonilla, F., and de Herreros, A.G. (2008). A natural antisense transcript regulates Zeb2/Sip1 gene expression during Snail1-induced epithelial-mesenchymal transition. Genes & development *22*, 756-769.

Bertozzi, D., Iurlaro, R., Sordet, O., Marinello, J., Zaffaroni, N., and Capranico, G. (2011). Characterization of novel antisense HIF-1alpha transcripts in human cancers. Cell cycle *10*, 3189-3197.

Bourdon, J.C. (2007). p53 Family isoforms. Current pharmaceutical biotechnology *8*, 332-336.

Bussemakers, M.J., van Bokhoven, A., Verhaegh, G.W., Smit, F.P., Karthaus, H.F., Schalken, J.A., Debruyne, F.M., Ru, N., and Isaacs, W.B. (1999). DD3: a new prostate-specific gene, highly overexpressed in prostate cancer. Cancer research *59*, 5975-5979.

Carrell, D.T. (2013). Aberrant methylation of the H19 imprinting control region may increase the risk of spontaneous abortion. Epigenomics *5*, 23-24.

Chau, Y.M., Pando, S., and Taylor, H.S. (2002). HOXA11 silencing and endogenous HOXA11 antisense ribonucleic acid in the uterine endometrium. The Journal of clinical endocrinology and metabolism *87*, 2674-2680.

Chung, S., Nakagawa, H., Uemura, M., Piao, L., Ashikawa, K., Hosono, N., Takata, R., Akamatsu, S., Kawaguchi, T., Morizono, T., *et al.* (2011). Association of a novel long non-coding RNA in 8q24 with prostate cancer susceptibility. Cancer science *102*, 245-252.

Corcoran, M.M., Hammarsund, M., Zhu, C., Lerner, M., Kapanadze, B., Wilson, B., Larsson, C., Forsberg, L., Ibbotson, R.E., Einhorn, S., *et al.* (2004). DLEU2 encodes an antisense RNA for the putative bicistronic RFP2/LEU5 gene in humans and mouse. Genes, chromosomes & cancer *40*, 285-297.

Cui, L., Xie, X.Y., Wang, H., Chen, X.L., Liu, S.L., and Hu, L.N. (2013). [Expression of long non-coding RNA HOTAIR mRNA in ovarian cancer]. Sichuan da xue xue bao Yi xue ban = Journal of Sichuan University Medical science edition *44*, 57-59.

Deng, Z., Norseen, J., Wiedmer, A., Riethman, H., and Lieberman, P.M. (2009). TERRA RNA binding to TRF2 facilitates heterochromatin formation and ORC recruitment at telomeres. Molecular cell *35*, 403-413.

Du, Y., Kong, G., You, X., Zhang, S., Zhang, T., Gao, Y., Ye, L., and Zhang, X. (2012). Elevation of highly up-regulated in liver cancer (HULC) by hepatitis B virus X protein promotes hepatoma cell proliferation via down-regulating p18. The Journal of biological chemistry *287*, 26302-26311.

Feng, J., Bi, C., Clark, B.S., Mady, R., Shah, P., and Kohtz, J.D. (2006). The Evf-2 noncoding RNA is transcribed from the Dlx-5/6 ultraconserved region and functions as a Dlx-2 transcriptional coactivator. Genes & development *20*, 1470-1484.

Francke, U. (1998). Imprinted genes in the Prader-Willi deletion. Novartis Foundation symposium *214*, 264-275; discussion 275-269.

Garcia-Claver, A., Lorente, M., Mur, P., Campos-Martin, Y., Mollejo, M., Velasco, G., and Melendez, B. (2013). Gene expression changes associated with erlotinib response in glioma cell lines. European journal of cancer *49*, 1641-1653.

Garrels, W., Kues, W.B., Herrmann, D., Holler, S., Baulain, U., and Niemann, H. (2012). Ectopic expression of human telomerase RNA component results in increased telomerase activity and elongated telomeres in bovine blastocysts. Biology of reproduction *87*, 95.
Glasgow, E., Ryu, S.L., Yamashita, M., Zhang, B.J., Mutsuga, N., and Gainer, H. (2005). APeg3, a novel paternally expressed gene 3 antisense RNA transcript specifically expressed in vasopressinergic magnocellular neurons in the rat supraoptic nucleus. Brain research Molecular brain research *137*, 143-151.
Goode, E.L., Chenevix-Trench, G., Song, H., Ramus, S.J., Notaridou, M., Lawrenson, K., Widschwendter, M., Vierkant, R.A., Larson, M.C., Kjaer, S.K., *et al.* (2010). A genome-wide association study identifies susceptibility loci for ovarian cancer at 2q31 and 8q24. Nature genetics *42*, 874-879.
Guo, X., Lin, M., Rockowitz, S., Lachman, H.M., and Zheng, D. (2014). Characterization of human pseudogene-derived non-coding RNAs for functional potential. PloS one *9*, e93972.
Hancock, A.L., Brown, K.W., Moorwood, K., Moon, H., Holmgren, C., Mardikar, S.H., Dallosso, A.R., Klenova, E., Loukinov, D., Ohlsson, R., *et al.* (2007). A CTCF-binding silencer regulates the imprinted genes AWT1 and WT1-AS and exhibits sequential epigenetic defects during Wilms' tumourigenesis. Human molecular genetics *16*, 343-354.
Harrow, J., Frankish, A., Gonzalez, J.M., Tapanari, E., Diekhans, M., Kokocinski, F., Aken, B.L., Barrell, D., Zadissa, A., Searle, S., *et al.* (2012). GENCODE: the reference human genome annotation for The ENCODE Project. Genome research *22*, 1760-1774.
He, H., Nagy, R., Liyanarachchi, S., Jiao, H., Li, W., Suster, S., Kere, J., and de la Chapelle, A. (2009). A susceptibility locus for papillary thyroid carcinoma on chromosome 8q24. Cancer research *69*, 625-631.
Hung, T., Wang, Y., Lin, M.F., Koegel, A.K., Kotake, Y., Grant, G.D., Horlings, H.M., Shah, N., Umbricht, C., Wang, P., *et al.* (2011). Extensive and coordinated transcription of noncoding RNAs within cell-cycle promoters. Nature genetics *43*, 621-629.
Ip, J.Y., and Nakagawa, S. (2012). Long non-coding RNAs in nuclear bodies. Development, growth & differentiation *54*, 44-54.
Khaitan, D., Dinger, M.E., Mazar, J., Crawford, J., Smith, M.A., Mattick, J.S., and Perera, R.J. (2011). The melanoma-upregulated long noncoding RNA SPRY4-IT1 modulates apoptosis and invasion. Cancer research *71*, 3852-3862.
Kuiper, R.P., Schepens, M., Thijssen, J., van Asseldonk, M., van den Berg, E., Bridge, J., Schuuring, E., Schoenmakers, E.F., and van Kessel, A.G. (2003). Upregulation of the transcription factor TFEB in t(6;11)(p21;q13)-positive renal cell carcinomas due to promoter substitution. Human molecular genetics *12*, 1661-1669.
Lerner, M., Harada, M., Loven, J., Castro, J., Davis, Z., Oscier, D., Henriksson, M., Sangfelt, O., Grander, D., and Corcoran, M.M. (2009). DLEU2, frequently deleted in malignancy, functions as a critical host gene of the cell cycle inhibitory microRNAs miR-15a and miR-16-1. Experimental cell research *315*, 2941-2952.
Li, J., Witte, D.P., Van Dyke, T., and Askew, D.S. (1997). Expression of the putative proto-oncogene His-1 in normal and neoplastic tissues. The American journal of pathology *150*, 1297-1305.
Liu, A.Y., Torchia, B.S., Migeon, B.R., and Siliciano, R.F. (1997). The human NTT gene: identification of a novel 17-kb noncoding nuclear RNA expressed in activated CD4+ T cells. Genomics *39*, 171-184.
Liu, Q., Huang, J., Zhou, N., Zhang, Z., Zhang, A., Lu, Z., Wu, F., and Mo, Y.Y. (2013). LncRNA loc285194 is a p53-regulated tumor suppressor. Nucleic acids research *41*, 4976-4987.
Madamanchi, N.R., Hu, Z.Y., Li, F., Horaist, C., Moon, S.K., Patterson, C., Runge, M.S., Ruef, J., Fritz, P.H., and Aaron, J. (2002). A noncoding RNA regulates human protease-activated receptor-1 gene during embryogenesis. Biochimica et biophysica acta *1576*, 237-245.
Massone, S., Ciarlo, E., Vella, S., Nizzari, M., Florio, T., Russo, C., Cancedda, R., and Pagano, A. (2012). NDM29, a RNA polymerase III-dependent non coding RNA, promotes amyloidogenic processing of APP and amyloid beta secretion. Biochimica et biophysica acta *1823*, 1170-1177.
Migeon, B.R. (2003). Is Tsix repression of Xist specific to mouse? Nature genetics *33*, 337; author reply 337-338.

Monti, L., Cinquetti, R., Guffanti, A., Nicassio, F., Cremona, M., Lavorgna, G., Bianchi, F., Vignati, F., Cittaro, D., Taramelli, R., *et al.* (2009). In silico prediction and experimental validation of natural antisense transcripts in two cancer-associated regions of human chromosome 6. International journal of oncology *34*, 1099-1108.
Motomiya, Y., Higashimoto, Y., Uji, Y., Suenaga, G., and Ando, Y. (2015). C-terminal unfolding of an amyloidogenic beta2-microglobulin fragment: DeltaN6beta2-microglobulin. Amyloid : the international journal of experimental and clinical investigation : the official journal of the International Society of Amyloidosis *22*, 54-60.
Nguewa, P.A., Agorreta, J., Blanco, D., Lozano, M.D., Gomez-Roman, J., Sanchez, B.A., Valles, I., Pajares, M.J., Pio, R., Rodriguez, M.J., *et al.* (2008). Identification of importin 8 (IPO8) as the most accurate reference gene for the clinicopathological analysis of lung specimens. BMC molecular biology *9*, 103.
Nie, Y., Liu, X., Qu, S., Song, E., Zou, H., and Gong, C. (2013). Long non-coding RNA HOTAIR is an independent prognostic marker for nasopharyngeal carcinoma progression and survival. Cancer science *104*, 458-464.
Niland, C.N., Merry, C.R., and Khalil, A.M. (2012). Emerging Roles for Long Non-Coding RNAs in Cancer and Neurological Disorders. Frontiers in genetics *3*, 25.
Novikova, I.V., Hennelly, S.P., and Sanbonmatsu, K.Y. (2012). Structural architecture of the human long non-coding RNA, steroid receptor RNA activator. Nucleic acids research *40*, 5034-5051.
Oh, J.H., Yang, J.O., Hahn, Y., Kim, M.R., Byun, S.S., Jeon, Y.J., Kim, J.M., Song, K.S., Noh, S.M., Kim, S., *et al.* (2005). Transcriptome analysis of human gastric cancer. Mammalian genome : official journal of the International Mammalian Genome Society *16*, 942-954.
Pasmant, E., Laurendeau, I., Heron, D., Vidaud, M., Vidaud, D., and Bieche, I. (2007). Characterization of a germ-line deletion, including the entire INK4/ARF locus, in a melanoma-neural system tumor family: identification of ANRIL, an antisense noncoding RNA whose expression coclusters with ARF. Cancer research *67*, 3963-3969.
Potter, S.S., and Branford, W.W. (1998). Evolutionary conservation and tissue-specific processing of Hoxa 11 antisense transcripts. Mammalian genome : official journal of the International Mammalian Genome Society *9*, 799-806.
Qiao, H.P., Gao, W.S., Huo, J.X., and Yang, Z.S. (2013). Long non-coding RNA GAS5 functions as a tumor suppressor in renal cell carcinoma. Asian Pacific journal of cancer prevention : APJCP *14*, 1077-1082.
Radulovich, N., Pham, N.A., Strumpf, D., Leung, L., Xie, W., Jurisica, I., and Tsao, M.S. (2010). Differential roles of cyclin D1 and D3 in pancreatic ductal adenocarcinoma. Molecular cancer *9*, 24.
Rintala-Maki, N.D., and Sutherland, L.C. (2009). Identification and characterisation of a novel antisense non-coding RNA from the RBM5 gene locus. Gene *445*, 7-16.
Rosenbluh, J., Nijhawan, D., Chen, Z., Wong, K.K., Masutomi, K., and Hahn, W.C. (2011). RMRP is a non-coding RNA essential for early murine development. PloS one *6*, e26270.
Sanders, A.M., Edwards, H.M., Jr., and Rowland, G.N., 3rd (1992). Calcium and phosphorus requirements of the very young turkey as determined by response surface analysis. The British journal of nutrition *67*, 421-435.
Schwartz, J.C., Younger, S.T., Nguyen, N.B., Hardy, D.B., Monia, B.P., Corey, D.R., and Janowski, B.A. (2008). Antisense transcripts are targets for activating small RNAs. Nature structural & molecular biology *15*, 842-848.
Sidiropoulos, M., Chang, A., Jung, K., and Diamandis, E.P. (2001). Expression and regulation of prostate androgen regulated transcript-1 (PART-1) and identification of differential expression in prostatic cancer. British journal of cancer *85*, 393-397.
Song, X., Wang, X., Arai, S., and Kurokawa, R. (2012). Promoter-associated noncoding RNA from the CCND1 promoter. Methods in molecular biology *809*, 609-622.
Sonkoly, E., Bata-Csorgo, Z., Pivarcsi, A., Polyanka, H., Kenderessy-Szabo, A., Molnar, G., Szentpali, K., Bari, L., Megyeri, K., Mandi, Y., *et al.* (2005). Identification and characterization of a novel, psoriasis

susceptibility-related noncoding RNA gene, PRINS. The Journal of biological chemistry *280*, 24159-24167.
Spigoni, G., Gedressi, C., and Mallamaci, A. (2010). Regulation of Emx2 expression by antisense transcripts in murine cortico-cerebral precursors. PloS one *5*, e8658.
Strausberg, R.L., Feingold, E.A., Grouse, L.H., Derge, J.G., Klausner, R.D., Collins, F.S., Wagner, L., Shenmen, C.M., Schuler, G.D., Altschul, S.F., *et al.* (2002). Generation and initial analysis of more than 15,000 full-length human and mouse cDNA sequences. Proceedings of the National Academy of Sciences of the United States of America *99*, 16899-16903.
Suo, G., Han, J., Wang, X., Zhang, J., Zhao, Y., Zhao, Y., and Dai, J. (2005). Oct4 pseudogenes are transcribed in cancers. Biochemical and biophysical research communications *337*, 1047-1051.
Szafron, L.M., Balcerak, A., Grzybowska, E.A., Pienkowska-Grela, B., Felisiak-Golabek, A., Podgorska, A., Kulesza, M., Nowak, N., Pomorski, P., Wysocki, J., *et al.* (2015). The Novel Gene CRNDE Encodes a Nuclear Peptide (CRNDEP) Which Is Overexpressed in Highly Proliferating Tissues. PloS one *10*, e0127475.
Wang, P., Ren, Z., and Sun, P. (2012). Overexpression of the long non-coding RNA MEG3 impairs in vitro glioma cell proliferation. Journal of cellular biochemistry *113*, 1868-1874.
Wang, X.S., Zhang, Z., Wang, H.C., Cai, J.L., Xu, Q.W., Li, M.Q., Chen, Y.C., Qian, X.P., Lu, T.J., Yu, L.Z., *et al.* (2006). Rapid identification of UCA1 as a very sensitive and specific unique marker for human bladder carcinoma. Clinical cancer research : an official journal of the American Association for Cancer Research *12*, 4851-4858.
Wang, Y., Wang, Y., Li, J., Zhang, Y., Yin, H., and Han, B. (2015). CRNDE, a long-noncoding RNA, promotes glioma cell growth and invasion through mTOR signaling. Cancer letters *367*, 122-128.
Wey, E., Lyons, G.E., and Schafer, B.W. (1994). A human POU domain gene, mPOU, is expressed in developing brain and specific adult tissues. European journal of biochemistry / FEBS *220*, 753-762.
Willingham, A.T., Orth, A.P., Batalov, S., Peters, E.C., Wen, B.G., Aza-Blanc, P., Hogenesch, J.B., and Schultz, P.G. (2005). A strategy for probing the function of noncoding RNAs finds a repressor of NFAT. Science *309*, 1570-1573.
Xue, Y., Wang, M., Kang, M., Wang, Q., Wu, B., Chu, H., Zhong, D., Qin, C., Yin, C., Zhang, Z., *et al.* (2013). Association between lncrna PCGEM1 polymorphisms and prostate cancer risk. Prostate cancer and prostatic diseases *16*, 139-144, S131.
Yang, F., Zhang, L., Huo, X.S., Yuan, J.H., Xu, D., Yuan, S.X., Zhu, N., Zhou, W.P., Yang, G.S., Wang, Y.Z., *et al.* (2011). Long noncoding RNA high expression in hepatocellular carcinoma facilitates tumor growth through enhancer of zeste homolog 2 in humans. Hepatology *54*, 1679-1689.
Yu, G., Yao, W., Gumireddy, K., Li, A., Wang, J., Xiao, W., Chen, K., Xiao, H., Li, H., Tang, K., *et al.* (2014). Pseudogene PTENP1 functions as a competing endogenous RNA to suppress clear-cell renal cell carcinoma progression. Molecular cancer therapeutics *13*, 3086-3097.
Yu, M., Ohira, M., Li, Y., Niizuma, H., Oo, M.L., Zhu, Y., Ozaki, T., Isogai, E., Nakamura, Y., Koda, T., *et al.* (2009). High expression of ncRAN, a novel non-coding RNA mapped to chromosome 17q25.1, is associated with poor prognosis in neuroblastoma. International journal of oncology *34*, 931-938.
Zhang, Q., Chen, C.Y., Yedavalli, V.S., and Jeang, K.T. (2013a). NEAT1 long noncoding RNA and paraspeckle bodies modulate HIV-1 posttranscriptional expression. mBio *4*, e00596-00512.
Zhang, W., Huang, C., Gong, Z., Zhao, Y., Tang, K., Li, X., Fan, S., Shi, L., Li, X., Zhang, P., *et al.* (2013b). Expression of LINC00312, a long intergenic non-coding RNA, is negatively correlated with tumor size but positively correlated with lymph node metastasis in nasopharyngeal carcinoma. Journal of molecular histology *44*, 545-554.
Zhang, X., Lian, Z., Padden, C., Gerstein, M.B., Rozowsky, J., Snyder, M., Gingeras, T.R., Kapranov, P., Weissman, S.M., and Newburger, P.E. (2009). A myelopoiesis-associated regulatory intergenic noncoding RNA transcript within the human HOXA cluster. Blood *113*, 2526-2534.
Zhang, X., Sun, S., Pu, J.K., Tsang, A.C., Lee, D., Man, V.O., Lui, W.M., Wong, S.T., and Leung, G.K. (2012). Long non-coding RNA expression profiles predict clinical phenotypes in glioma. Neurobiology of disease *48*, 1-8.

Zhang, X.M., Wang, X.Y., Sheng, S.R., Wang, J.R., and Li, J. (2003). Expression of tumor related genes NGX6, NAG-7, BRD7 in gastric and colorectal cancer. World journal of gastroenterology *9*, 1729-1733.
Zhou, L., Lim, Q.E., Wan, G., and Too, H.P. (2010). Normalization with genes encoding ribosomal proteins but not GAPDH provides an accurate quantification of gene expressions in neuronal differentiation of PC12 cells. BMC genomics *11*, 75.